Front. Phys., 2012, 7(2): 165–174
DOI 10.1007/s11467-011-0190-3

REVIEW ARTICLE

Electron transport properties of three-dimensional topological insulators

Yong-qing Li[1,†], **Ke-hui Wu**[1,*], **Jun-ren Shi**[2], **Xin-cheng Xie**[2,1]

[1] *Institute of Physics, Chinese Academy of Sciences, Beijing 100190, China*
[2] *International Center for Quantum Materials, Peking University, Beijing 100871, China*
E-mail: †*yqli@iphy.ac.cn*, **khwu@iphy.ac.cn*

Received March 30, 2011; accepted April 20, 2011

We review experimental advances in the study of the electron transport in three-dimensional topological insulators with emphasis on experiments that attempted to identify the surface transport. Recent results on transport properties of topological insulator thin films will be discussed in the context of weak antilocalization and electron–electron interactions. Current status of gate-voltage control of the chemical potential in topological insulators will also be described.

Keywords topological insulator, electron transport, localization, electron–electron interaction, spin–orbit coupling

PACS numbers 72.15.Rn, 73.25.+i, 03.65.Vf, 71.70.Ej

Contents

1 Introduction 165
2 Quantum oscillations in TI single crystals 166
3 Phase-coherent phenomena in TI nanoribbons 167
4 Transport properties of TI thin films 167
4.1 Growth of TI thin films with MBE 167
4.2 Gate-voltage tuning of chemical potential 168
4.3 Magnetoconductivity and weak antilocalization 169
4.4 Temperature dependence and electron–electron interactions 171
5 Summary and outlook 172
Acknowledgements 172
References 172

1 Introduction

Electron transport played a decisive role in the discovery of two-dimensional (2D) topological states of matter, which were unveiled by observations of the quantum Hall effect in 1980 [1] and the quantum spin Hall effect in 2007 [2–5]. In contrast, early evidence for the existence of their three-dimensional counterparts, 3D topological insulators [6–9], were gathered with surface probe techniques such as angular resolved photoemission spectroscopy (ARPES) [10–12] and scanning tunneling microscopy (STM) [13, 14]. By definition, a 3D topological insulator (TI) has an insulating bulk and conducting surfaces, on which resides a 2D system of Dirac fermions featuring continuous energy spectrum with linear dispersion [15–17]. Given the experience gained from intensive studies of graphene, another Dirac electron system (though topologically trivial) [18], one may expect that the unique transport properties of the surface states would not be very difficult to observe. It turns out that most of the fascinating properties predicted for TI still remain to be observed despite a lot of effort. The difficulty arises from the fact that the bulk of any TI known to date is not completely insulating even at very low temperatures. Nevertheless, remarkable progress has been made in the last couple of years in improving the carrier mobility, suppressing the bulk conductivity, identifying the surface state transport, as well as engineering suitable structures for electrical gating.

Here we review advances in the studies of transport properties of TI. We do not intend to make it exhaustive. We rather mainly focus on the experiments related to the surface state transport carried out at the Institute of Physics (IOP) and elsewhere. This article is organized as follows. Section 2 summarizes the advances in synthesis of high quality single crystals and the quantum oscillation experiments revealing the surface transport. In the next section the phase coherent transport in TI nanoribbons will be discussed briefly. Section 4 is the main part of this article. It describes the progress in the epitax-

©Higher Education Press and Springer-Verlag Berlin Heidelberg 2012

ial growth of TI thin films, electrical tuning of chemical potential and the related transport measurements. The experimental results will be discussed in the context of weak antilocalization and electron-electron interactions. Finally, a brief summary and outlook will be given in Section 5.

2 Quantum oscillations in TI single crystals

When a material with sufficiently high carrier mobility is subjected to a magnetic field, the Landau quantization of its energy spectrum leads to periodic oscillations in the magnetoresistance with $1/B$, the inverse of the magnetic field. This is the Shubnikov-de Haas (SdH) effect, first observed in bismuth single crystals in 1930. The SdH oscillations and their close cousin, the de Haas-van Alphen (dHvA) oscillations, have since become important tools for determination of the Fermi surfaces of various materials [19]. The frequency of such quantum oscillations follows the Onsager relation, $F = \frac{1}{\Delta(1/B)} = \frac{\hbar}{2\pi e} A_{\mathrm{FS}}$. Here A_{FS} is the extremal cross-sectional area of the Fermi surface for a 3D material, and it turns into the area enclosed by the Fermi circle in 2D. SdH oscillations in a 2D electron system (2DES) are dependent only on $B_{\perp}$, the perpendicular component of the magnetic field. It is therefore possible to differentiate a 2DES from bulk states by measuring the resistance oscillations in tilted magnetic fields.

Studies of the quantum oscillations in TI materials can actually be dated back to several decades ago. For instance, Köhler *et al.* carried out a series of systematic measurements of Bi_2Se_3 and Bi_2Te_3 in 1970s [20–24]. The knowledge gained at that time, though without the concept of TI, is still of great value today. The evidence for quantum oscillations of 2D character in a TI was first reported by Taskin and Ando, who measured dHvA oscillations in $Bi_{1-x}Sb_x$ [25]. This binary alloy is however not favored in TI research because of a complicated electronic structure, which comprises five Dirac cones inside the first Brillouin zone [10]. In contrast, the second generation of TIs (Bi_2Se_3, Bi_2Te_3, and Sb_2Te_3) are characterized by a single Dirac cone [11, 12, 26]. They have become favorite systems for both theoretical and experimental research. It is not difficult to synthesize Bi_2Se_3 and Bi_2Te_3 single crystals harboring SdH oscillations in the bulk. However, observation of the oscillations from the surface states turned out to be very challenging. Only a few groups have so far succeeded in obtaining clear evidence for SdH oscillations of 2D origin.

Bi_2Se_3 has a bulk band gap of about 0.3 eV, the largest among all known binary TIs. More importantly, its Dirac point is located inside the gap [26]. This feature is highly desirable for experiments that require the Fermi energy to be placed at or very close to the Dirac point (e.g., detection of Majorana fermions) [27–29]. The undoped Bi_2Se_3 is usually n-type and has substantial bulk conductivity due to selenium vacancies [30]. Compensation doping with Ca and Mg has been used to reduce the electron concentration and shown to be able to make the samples p-type [30, 31]. This technique, however, only raises the bulk resistivity up to several mΩ·cm [30]. SdH oscillations from the surface states have not been observed in the compensation-doped samples. On the other hand, Butch *et al.* managed to lower the electron density of undoped Bi_2Se_3 single crystals to about $10^{16}\,\mathrm{cm}^{-3}$ and improve the mobilities to over $2\times10^4\,\mathrm{cm}^2/(\mathrm{V{\cdot}s})$ [32]. Nevertheless, they were only able to observe the quantum oscillations from the bulk. The absence of the surface signal suggests a lower mobility of the surface carriers than that of the bulk. It is attributed to strong surface scattering [32].

An important step forward was achieved by Analytis *et al.* in 2010 [33]. They showed that the isovalent substitution of Bi with Sb can reduce the defect density in Bi_2Se_3 and lower the electron density to about $3\times10^{16}\,\mathrm{cm}^{-2}$. Ultrahigh magnetic fields (up to 55 T) brought the transport in the 3D quantum limit. The observed magneto-oscillations are periodic in $1/B_{\perp}$, regardless of the sample tilt angle. They also found that the oscillations can be diminished by exposure of the sample to atmosphere. These features build a strong case for a surface origin of the SdH oscillations. An effective mass of $0.11m_e$ was deduced from the temperature dependence measurements. The authors attribute it to the magnetic field enhanced cyclotron mass. This value is, however, very close to the effective mass of the bulk conduction band ($0.12m_e$) [22]. In a recent ARPES experiment, Bianchi *et al.* observed coexistence of topologically trivial quantum well states with the surface Dirac fermions. They suggest a downward band bending near the surface of Bi_2Se_3 [34]. Concern has to be raised if similar surface accumulation also takes place in the samples used in the transport measurements. However, it should be noted that an opposite band bending was proposed in an earlier work that combined ARPES and transport measurements [35].

Significant progress was also made on Bi_2Te_3. Unlike Bi_2Se_3, Bi_2Te_3 can be made either n-type or p-type without doping [30]. Qu *et al.* measured Bi_2Te_3 single crystals with resistivities of 4–12 mΩ·cm at low T in tilted fields. They concluded that the observed SdH oscillations are of surface origin [36]. In a subsequent experiment, Xiu *et al.* made similar observations in a Bi_2Te_3 nanoribbon prepared with a wet chemistry method [37]. They managed to tune SdH oscilliations with a SiO_2/Si backgate. The deduced cyclotron mass was found to increase from $0.11m_e$ to $0.13m_e$ as the gate voltage is varied from +20 V to +80 V. This trend is consistent with the increase in the SdH frequency (and hence the Fermi wavevector of the surface Dirac electrons) as the gate

voltage increases. The surface carrier mobility based on the analysis of SdH signals is estimated to be $\sim 5\times10^3\,\mathrm{cm}^2/(\mathrm{V{\cdot}s})$, about three times the value obtained by Analytis *et al.* in Bi_2Se_3 [33]. Nevertheless, the total conductivity of the Bi_2Te_3 nanoribbon decreases as the gate voltage gets larger. This indicates that the p-type bulk conductivity still plays a significant role in the transport.

Recently two groups made remarkable contributions to the suppression of the bulk conductivity in TI materials [38, 39]. They synthesized high quality Bi_2Te_2Se single crystals with improved melt-cooling methods. Ren *et al.* [38] reported bulk resistivities exceeding $1\,\Omega{\cdot}$cm and variable-range-hopping transport at low temperatures. SdH oscillations were shown to be of surface origin. Xiong *et al.* [39] subsequently reported that the resistivity of Bi_2Te_2Se can reach as high as $6\,\Omega{\cdot}$cm, and convincing surface SdH oscillations were also observed. Both groups have attempted to extract the $1/B$ values for integer fillings of Landau levels (LL). This could lead to direct evidence for the Dirac energy spectrum if those values are accurate enough to confirm the following Landau level filling relation: $1/B=(\nu+1/2)e/(n_{2\mathrm{D}}h)$, where ν is the filling factor, and $n_{2\mathrm{D}}$ is the carrier density on the surface, and the offset 1/2 originates from the Berry phase of the Dirac fermions [40, 41]. Such effort is, however, complicated by the large Zeeman energy as well as deviation from linear dispersion in this class of materials [42].

3 Phase-coherent phenomena in TI nanoribbons

At low temperatures, electron's wavefunction can remain coherent even after many elastic scattering events. A beautiful manifestation of the phase coherence was conceived by Altshuler, Aronov and Spivak (AAS) in 1981 [43]. They considered the interference between electrons traveling in two identical but time-reversed paths with a magnetic flux Φ piercing through. Based on a seminal work by Aharonov and Bohm in 1959 [44], the phase difference between the two paths is $4\pi\Phi/\Phi_0$, where $\Phi_0=h/e$ is the flux quantum. The consequence is that constructive interference occurs in a period of $h/(2e)$ as the magnetic field is varied. AAS oscillations were soon observed by measuring the resistance along a thin glass fiber coated with Mg thin film [45]. A more modern demonstration of AAS oscillations was realized with carbon nanotubes [46]. If the surface transport on a TI is indeed isolated from the bulk conductivity, similar measurement of a nanowire-shaped sample could in principle provide an ideal probe for the surface transport. Peng *et al.* reported the first such experiment [47]. They observed magnetoresistance oscillations in a Bi_2Se_3 nanoribbon with a period of h/e instead of $h/(2e)$. This surprising result still remains to be understood. Two scenarios for h/e periodicity have been proposed theoretically [48, 49], but both predict conductivity maxima at odd multiples of $h/(2e)$, instead of the integer multiples of h/e observed in the experiment. It is noteworthy that similar h/e oscillations have also been observed in Bi_2Te_3 nanoribbons, but the FFT analyses yielded $h/(2e)$ periodicity in addition to the h/e oscillations [37, 50].

According to theory, AAS oscillations are possible with TI nanoribbons in the diffusive transport regime [48]. The electron spins on a TI surface are transversely locked to their translation momenta [51]. The Berry phase associated with the spin-helical structure causes destructive interference between the two time-reversed paths. This effect leads to a conductivity maximum at zero magnetic fields. Similar to early AAS experiments [45, 46], the h/e periodicity is expected to be suppressed in this regime because of ensemble average [52]. Experimental demonstration of the h/e or $h/(2e)$ oscillations with theoretically predicted features will be a major achievement, but the control of surface chemical potential and disorder strength could be a demanding task. Much work has to be done, both experimentally and theoretically, before the interference experiment can be established as a reliable method for identifying and characterizing the surface state transport on topological insulators.

4 Transport properties of TI thin films

Topological insulator thin films are attractive not only for future device applications, but also for the extra degrees of control offered by the low dimensionality. For instance, when a TI film is sufficiently thin, the coupling between the top and the bottom surface could result in a crossover from 3D to 2D topological states [53, 54]. TI thin films are also more suitable for gate-voltage control of the chemical potential than bulk materials. Such control is a necessary ingredient to observe various topological effects and explore novel device applications. Moreover, modern thin film growth technologies, such as molecular beam epitaxy (MBE), may eventually produce samples with carrier mobilities much higher than bulk crystals if further progress can be made in defect control, surface protection, as well as heterostructure engineering.

4.1 Growth of TI thin films with MBE

The growth of TI thin films with MBE was first reported by a few groups at the IOP and Tsinghua University [14, 55]. Since then, Bi_2Se_3 and Bi_2Te_3 thin films have been synthesized on many substrates including graphene/SiC [56–58], $SrTiO_3$ [59, 60], Al_2O_3 [62], Si [63, 64], ZnSe [61]

and GaAs [65]. Se- or Te-rich growth conditions were found to be important for realizing the layer-by-layer growth mode and obtaining the right stoichiometry [55]. A typical surface morphology is displayed in Fig. 1(a). It shows flat terraces of Bi_2Se_3 with step height of a quintuple layer (0.95 nm). If a Bi_2Se_3 film is sufficiently thick (e.g. 50 nm), the Fermi energy on the top surface could be located in the band gap according to an in situ ARPES experiment [56]. In contrast, the Fermi energy in the films thinner than 10 nm is often much higher than the conduction band minimum. The significant electron doping may come from the defects in the films and possibly in some cases charge transfer from the substrates. Nevertheless, the TI films grown with MBE have allowed for observation of the Landau level quantization in the surface states and also provided a direct evidence for the linear dispersion by using scanning tunneling spectroscopy [66]. Suppression of backscattering due to the Berry phase has been demonstrated by imaging standing waves scattered off nonmagnetic impurities on a Bi_2Te_3 thin film [14].

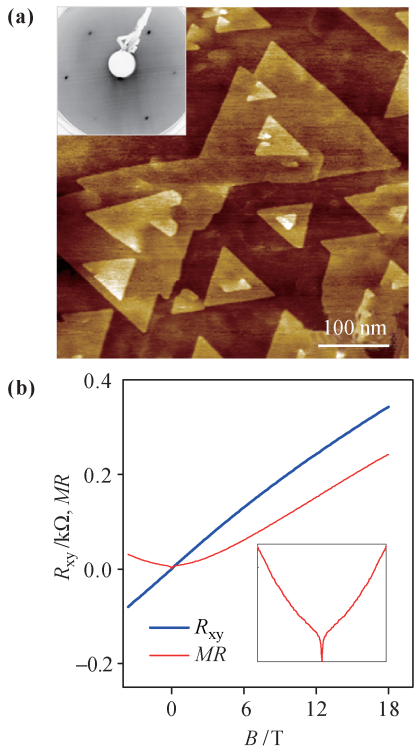

Fig. 1 **(a)** A typical STM image of Bi_2Se_3 thin films grown on $SrTiO_3(111)$ substrates. The low energy electron diffraction pattern is shown on the upper-left corner. Reproduced from Ref. [59], Copyright © 2010 American Physical Society. **(b)** Magnetoresistance (MR), defined as $MR = \rho_{xx}(B)/\rho_{xx}(0) - 1$, and Hall resistance, R_{xy}, of a Bi_2Se_3 thin film at $T = 1.2$ K. A close-up view of the MR between ±3 T is shown in the lower inset. Reproduced from Ref. [70].

Ex-situ transport measurements of the MBE-grown thin films have been carried out extensively by several groups [59, 65, 67–70]. All of the films showed n-type conductivity, even though some of them are coated with a Se or ZnS cap layer [67–69]. The electron densities extracted from Hall measurements are usually in the range of $(1–10)\times10^{13}\,cm^{-2}$. According to ARPES measurements, the top and bottom surface can only accommodate up to about $0.5\times10^{13}\,cm^{-2}$ even when the Fermi energy reaches the conduction band minimum [11, 35, 71]. This suggests the existence of a large number of bulk carriers (or quasi-2D carriers with parabolic dispersion) in most of these samples. The nonlinear Hall curve shown in Fig. 1(b) also suggests coexistence of multiple types of carriers, which are presumably the electrons at the top surface and the bottom surface (interface), as well as the conduction band electrons in the bulk. It was also found that exposure to atmosphere often leads to increase in electron density [72]. This is consistent with a previous ARPES experiment [35]. Since exposure to O_2 was shown to have an opposite effect, i.e. lowering the chemical potential in Bi_2Se_3 [31], the electron doping effect of atmosphere may be associated with the moisture. This conjecture is supported by a recent surface analysis work, but the mechanism related to the air exposure remains to be elucidated [73].

TI thin films can also be obtained with other methods, such as mechanical exfoliation from bulk single crystals [74, 75], vapor–solid deposition [47, 76] and wet chemistry growth [37]. These techniques, however, do not have good control over the thickness and the size of the samples. Ultrathin films (less than 20 nm thick), which are convenient for electrical gating, are still limited to micron sizes. This poses a serious limitation on transport studies as well as device applications. This difficulty can be circumvented with epitaxial thin films. However, SdH oscillations have never been observed in transport despite that the mobilities of epitaxial TI thin films have been improved to over $10^3\,cm^2/(V{\cdot}s)$ [60, 64].

4.2 Gate-voltage tuning of chemical potential

Precise tuning of the chemical potential in topological insulators is indispensable for many interesting experiments, such as searching Majorana fermions [27–29], observing quantum anomalous Hall effect [77], and detecting novel magnetoelectric effects [78, 79]. Many of these experiments prefer the chemical potential tuned with a backgate, because the top surface needs to be interfaced with structures of other materials. The most frequently used backgate dielectric is the SiO_2 layer on Si. It has been a workhorse for tuning the carrier densities in numerous low dimensional structures including graphene and carbon nanotubes. This technique, however, only offers charge tunability up to $1\times10^{13}\,cm^{-2}$, which is insufficient for most TI thin films currently available. Furthermore, the amorphous nature of SiO_2 is incompatible with the epitaxial growth. The application of SiO_2 dielectric to TIs has been limited to exfoliated nanoflakes or

synthesized nanoplates/nanoribbons. Effective tuning of the chemical potential on the top surface with a backgate had rarely been reported until recently [59, 60, 70, 75, 80], even though many groups have attempted electrical gating work on TI [37, 76, 81].

A method that can overcome the difficulty in gating has been developed at the IOP. It is based on the MBE growth of TI thin films on $SrTiO_3(111)$ substrates [59]. The high electric breakdown threshold of $SrTiO_3$ provides very large charge tuning capability. Its relative dielectric constant can exceed 10^4 at low T [82]. Applying a gate voltage of less than 200 V is sufficient to induce variations in the carrier density of at least $\pm 2\times 10^{13}\,\mathrm{cm}^{-2}$ [83]. Cautions have to be taken to avoid creating too much oxygen deficiency during the high temperature annealing of the substrates in order to preserve the high dielectric strength of $SrTiO_3$ [60].

Figure 2 shows the gate-voltage dependencies of the longitudinal resistivity (ρ_{xx}) at zero magnetic fields and the Hall resistance (R_{xy}) up to $B = 15$ T for a 10 nm thick Bi_2Se_3 film. It represents samples with the highest charge tunability obtained to date. As the gate voltage V_G is varied from +50 V to −86 V, R_{xy} increases by nearly one order of magnitude, corresponding to a change in electron density from about 3×10^{13} to $0.3\times 10^{13}\,\mathrm{cm}^{-2}$. At a slightly smaller gate voltage (~ -105 V), ρ_{xx} reaches the maximum, which is also enhanced by a factor of about 10. These features point to the existence of a certain amount of holes at the ρ_{xx} maximum. At larger negative gate voltages, the increasing hole density is manifested in the strongly nonlinear Hall curves and the reversal of the sign of R_{xy} at high fields. For the whole range of V_G, a minimum in the Hall constant is, however, not reached despite a trend pointing toward this. This implies that the Fermi energy at the top surface is still located above the Dirac point, whereas it drops below the Dirac point at the bottom surface. The corresponding band diagrams are shown in Fig. 2 (b, inset) for the two limiting cases, namely $0 > V_G > -50$ V and $V_G < -120$ V. Similar features were also observed by Checkelsky *et al.* in a Bi_2Se_3 thin flake exfoliated on a SiO_2/Si substrate [75]. In that work, the longitudinal resistivity in the Ca-doped sample was nevertheless only increased by a factor of about 3, much smaller than those obtained in epitaxial films on $SrTiO_3$. A maximum resistivity exceeding h/e^2 has been achieved by gating Bi_2Se_3 films grown on $SrTiO_3$ [59]. It is a very encouraging sign for much suppressed bulk conductivity induced by gating, even though the residue bulk conductivity cannot be completely ruled out.

4.3 Magnetoconductivity and weak antilocalization

As discussed in Section 3, the Berry phase associated with the spin-helical surface states suppresses the backscattering due to the destructive interference between two closed paths with time-reversal symmetry. It protects the electron system against the Anderson (weak) localization regardless of the strength of disorder. Such effect is referred to as weak antilocalization. The immunity to localization is expected to survive even when the electron–electron interactions are present [84]. The weak antilocalization can be brought out by measuring the magnetotransport. It causes negative

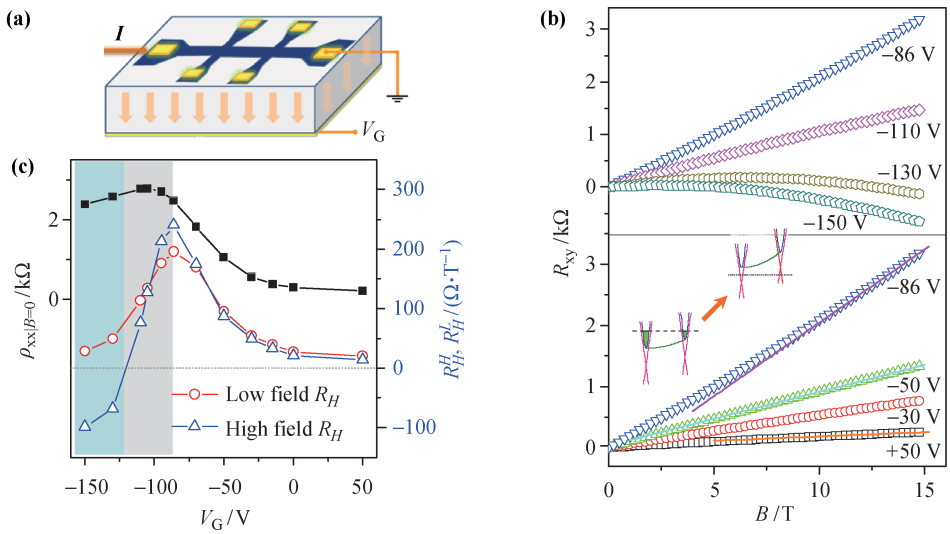

Fig. 2 **(a)** Sketch of a typical back-gated device used in this work. **(b)** Gate-voltage dependence of the Hall resistance R_{xy} for B up to 15 T. The bottom panel shows that R_{xy} increases as the gate voltage V_G is decreases from +50 V to −86 V. The solid lines are linear fits to R_{xy} in high magnetic fields (B = 13.5–15 T). The top panel shows R_{xy} decrease as V_G is reduced further from −86 V. The high field Hall resistances become negative for $V_G = -130$ V and −150 V. The inset shows two band diagrams for small (*left*) and large (*right*) negative gate voltages. **(c)** Gate-voltage dependencies of the low field Hall coefficient (R_H^L, *open circles*), the high field Hall coefficient (R_H^H, *open triangles*), and the longitudinal resistivity at $B = 0$ ($\rho_{xx}|_{B=0}$, *solid squares*). The main part of the figure is reproduced from Ref. [60], Copyright © 2011 Wiley-VCH Verlag GmbH & Co. KGaA.

magnetoconductivity due to the broken time-reversal symmetry in perpendicular magnetic fields. Following the work of McCann *et al.* on graphene [85], the magnetoconductivity can be written as

$$\Delta\sigma(B) \simeq -\alpha \cdot \frac{e^2}{\pi h}\left[\psi\left(\frac{1}{2}+\frac{B_\phi}{B}\right)-\ln\left(\frac{B_\phi}{B}\right)\right] \quad (1)$$

Here ψ is the digamma function, $B_\phi = \hbar/(4De\tau_\phi)$ is a characteristic field related to the electron dephasing time τ_ϕ, D is the diffusion constant, and the coefficient α takes a value of 1/2 for transport on one TI surface [86].

The weak antilocalization is not limited to the Dirac fermion systems alone. It also exists in traditional 2D electron systems with spin–orbit coupling (SOC), such as Au and InSb thin films. The corresponding magnetotransport has been extensively studied [87, 88]. The correction to magnetoconductivity is described by Hikami-Larkin–Nagaoka equation [89]

$$\begin{aligned}\Delta\sigma(B) = &-\frac{1}{2}\cdot\frac{e^2}{\pi h}\left[\psi\left(\frac{1}{2}+\frac{B_\phi}{B}\right)-\ln\left(\frac{B_\phi}{B}\right)\right]\\ &+\frac{3}{2}\cdot\frac{e^2}{\pi h}\left[\psi\left(\frac{1}{2}+\frac{B^*_{\rm so}}{B}\right)-\ln\left(\frac{B^*_{\rm so}}{B}\right)\right]\\ &-\frac{e^2}{\pi h}\left[\psi\left(\frac{1}{2}+\frac{B^*_{\rm e}}{B}\right)-\ln\left(\frac{B^*_{\rm e}}{B}\right)\right] \quad (2)\end{aligned}$$

with $B_{\rm so} = \hbar/(4De\tau_{\rm so})$, $B_{\rm e} = \hbar/(4De\tau_e)$, $B^*_{\rm so} = \frac{4}{3}B_{\rm so} + B_\phi$, $B^*_{\rm e} = B_{\rm e} + B_{\rm so}$, where $\tau_{\rm so}$ and τ_e are spin–orbit scattering time and elastic scattering time, respectively. The first term in Eq. (2) is related to the Cooperon in the spin singlet state. It is responsible for negative magnetoconductivity (weak antilocalization) at weak magnetic fields. The second (spin-triplet) term leads to positive magnetoconductivity (weak localization), and it becomes dominating as B increases. The last term determines the high field boundary for the range of magnetic fields where the logarithmic behavior resulting from the weak localization/antilocalization is observed. Generally speaking, this term is unimportant at low magnetic fields if the carrier mobility is low.

The crossover from the weak antilocalization to the weak localization with increasing B does not take place in the transport on one TI surface, which may be regarded as a 2DES with SOC of infinite strength. Eq. (1) (with $\alpha = 1/2$) thus gives a unified description of the magnetoconductivity for a TI surface and a topologically trivial 2DES with sufficiently strong SOC. The examples for the latter include many heavy metal systems such as Au, Pt and Bi thin films, which only show negative magnetoconductivity as a result of dominating SOC [87, 90, 91].

Magnetotransport properties have been measured in Bi_2Se_3 and Bi_2Te_3 thin films on various substrates [59, 67–69, 92]. All of them showed the negative magnetoconductivity without crossover to positive magnetoconductivity at large magnetic fields. For the samples of Hall bar geometries, which allow accurate determination of the conductivity, the data can be well fitted by Eq. (1) with α values close to 1/2 [59, 70, 92]. The electron densities in these samples are in the range of $0.8 \times 10^{13}\,{\rm cm}^{-2}$ to $8.6 \times 10^{13}\,{\rm cm}^{-2}$. As discussed above, the Fermi energy in this case is probably located in the bulk conduction band. If there is no upward band bending near the surface, significant mixing between the bulk and surface states is expected. This may account for the single-component transport described by Eq. (1) even though multiple types of carriers coexist in the samples. An alternative explanation is that both the surface states and the bulk carriers contribute independently, and the dephasing field for one of the components is much smaller than those of the others. However, this scenario requires independent conducting channels, which may be difficult to realize in the (unintentionally) n-doped samples without gating.

As discussed in Section 4.2, the transport at the top and bottom surface may be separated by applying a negative gate voltage. If the dephasing fields of these two conduction channels are comparable, fitting the magnetoconductivity data to Eq. (1) should yield α values deviating from 1/2. This was indeed observed in the recent experiments on 10-nm-thick Bi_2Se_3 films grown on $SrTiO_3$ [60, 70]. As shown in Fig. 3, when the electron density is high, corresponding to the Fermi energy located in the conduction band, the extracted α values are close to 1/2. Decreasing the gate voltage results in a much depleted bulk layer and hence separated conducting channels at the bottom and the top surfaces (see Fig. 2). The coefficient α increases as expected. At large negative voltages, α was found to be close to 1, indicating two independent conducting channels with comparable dephasing fields [70, 90].

The high field magnetoresistance is also noteworthy. As shown in Fig. 4, there exists a linear MR in a wide range of magnetic fields (5–15 T) for $V \geqslant -50$ V. It becomes much less pronounced for $V \leqslant -86$ V, when the surface conductivity presumably becomes more relevant. This suggests that the linear MR may not be treated as a unique signature for the transport of Dirac fermions [95]. Similar linear MR has also been reported in Bi_2Se_3 nanoribbons fabricated with chemical vapor deposition and Bi_2Te_3 single crystals [36, 97]. We note that a model based on strong inhomogeneity was proposed by Parish and Littlewood to account for similar MR observed in AgTe [94, 96]. However, it is unclear whether this model can be applied to such a large variety of materials prepared with so many different methods. The observed gate-voltage dependence of the slope of linear MR may be valuable to unveil the origin of the linear MR [60].

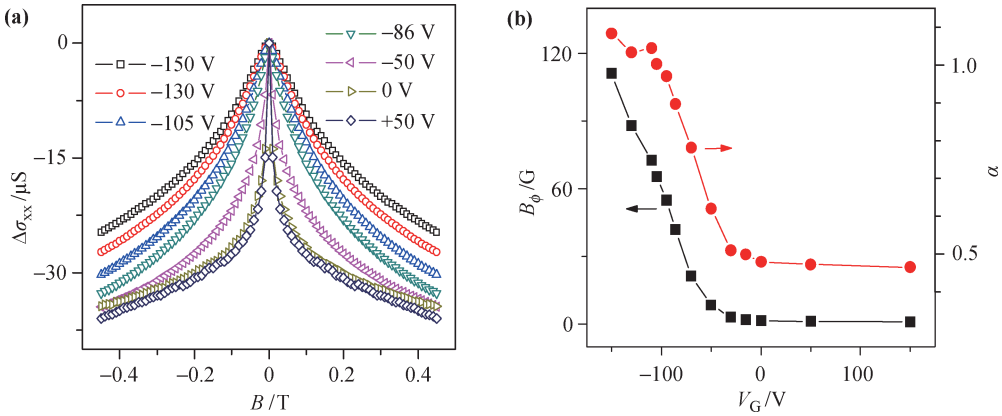

Fig. 3 **(a)** The gate-voltage dependence of the magnetoconductivity $\Delta\sigma(B)$ due to weak antilocalization. All of the data was taken at $T = 1.6$ K. Reproduced from Ref. [60], Copyright © 2011 Wiley-VCH Verlag GmbH & Co. KGaA. **(b)** Gate-voltage dependencies of dephasing field B_ϕ and coefficient α, which are obtained by fitting the $\Delta\sigma(B)$ to Eq. (1). For more detailed discussion of the relevant physics, please see Ref. [70].

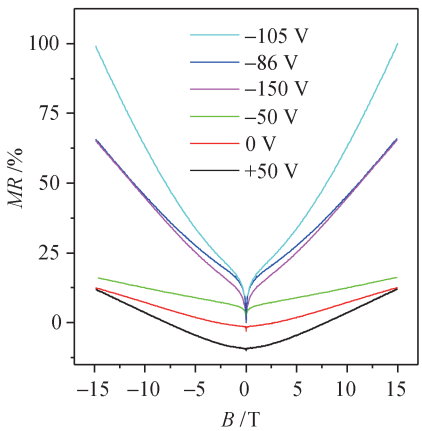

Fig. 4 The magnetoresistance at several gate voltages from +50 to −150 V. The MR curves for $V_G = +50$ V and 0 V are shifted downwards for clearer view. All of the data was taken at $T = 0.1$ K. Reprroduced from Ref. [60], Copyright © 2011 Wiley-VCH Verlag GmbH & Co. KGaA.

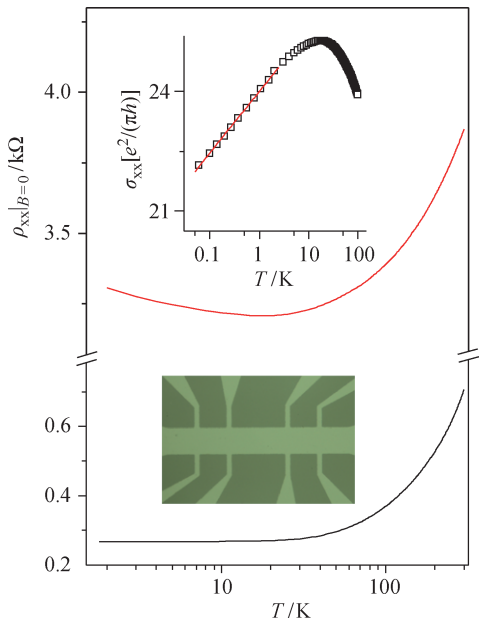

Fig. 5 Temperature dependence of the longitudinal resistivity ρ_{xx} at $B = 0$ for samples A (*top*) and B (*bottom*). The corresponding conductivity ($\sigma_{xx} = 1/\rho_{xx}$) for sample A follows a $\ln T$ type of dependence at low T. Part of the figure is reproduced from Ref. [70].

4.4 Temperature dependence and electron–electron interactions

Figure 5 displays temperature dependencies of the longitudinal resistance in two Bi_2Se_3 thin films grown with MBE. The resistance drops with decreasing temperature as a result of the reduced electron–phonon scatterings. This behavior persists only to a finite temperature (typically from a few K to about 20 K), below which ρ_{xx} eventually increases logarithmically with decreasing temperature [70]. Similar $\ln T$ dependence has also been reported in Bi_2Se_3 films by two other groups [68, 69]. All of the samples used in the T-dependent measurements reported so far have electron densities exceeding $2\times10^{13}\text{cm}^{-2}$. They are probably not in the so-called topological transport regime [71], since the contribution from the carriers of parabolic dispersion could be significant or even dominating in the transport.

The physics of the traditional, topologically trivial 2D system with strong SOC has been well understood. A latest discussion in the context of transport in TI is given in Ref. [84]. The scaling analysis predicts that the topologically trivial electron states are always localized regardless of the strength of disorder. Both electron–electron interactions and weak antilocalization leads to $\ln T$ type of temperature dependence, but their corrections to conductivity differ in magnitude and sign. The temperature dependent part of conductivity follows

$$\Delta\sigma(T)|_{B=0} = \left(1 - \frac{1}{2}\right)\frac{e^2}{\pi h}\ln T = \frac{e^2}{2\pi h}\ln T \qquad (3)$$

where the two coefficients (1 and −1/2) in the bracket are due to the effects of electron–electron interactions and weak antilocalization, respectively [84]. The interaction term (proportional to 1) is the singlet contribution

in the diffusion channel. It should be noted that for a 2D electron system with weak SOC, the e–e interaction term is proportional to $1 - \frac{3}{4}\tilde{F}^{\sigma}$, in which the second part comes from the triplet contribution in the diffusion channel [98, 99]. The $\tilde{F}^{\sigma}$ term is however suppressed for a system with strong SOC [84, 99–103]. The observed $\ln T$ dependencies are qualitatively in agreement with Eq. (3), even though the magnitude of the slope, defined as $\kappa = (\pi h/e^2)\mathrm{d}\sigma_{\mathrm{xx}}(T)/(\mathrm{d}\ln T)$, usually deviates from 1/2. This may be attributed to corrections in the Cooperon channel and possibly the existence of tiny amount of magnetic impurities in the samples [104].

It is also interesting to note that the e–e interactions do not lead to noticeable corrections to B-dependent part of the conductivity at low fields despite that the electron g-factor is quite large in bulk Bi_2Se_3 [22]. For 2D systems with weak SOC, a Zeeman split term in the diffusion channel is responsible for a field dependent correction proportional to $\widetilde{F}^{\sigma}$ [98, 99]. As discussed above, strong SOC can suppress the Zeeman correction. Tilted field measurements of the magnetoconductivity in a 10 nm thick Bi_2Se_3 thin film (with E_{F} located in the conduction band) have clearly shown that the Zeeman correction is indeed negligible for the range of magnetic fields relevant to the weak antilocalization [70].

As mentioned above, the temperature dependent measurements reported so far have been limited to samples with Fermi energy presumably located in the conduction band. It will be of great interest to carry out such measurements in samples where the surface state conductivity plays a dominating role. This may eventually render a direct evidence for the immunity to localization of the surface Dirac fermions.

5 Summary and outlook

In the past few years we have witnessed remarkable progress in many aspects of transport studies of the 3D topological insulators. These include synthesis of high quality single crystals for suppression of the bulk conductivity and quantum oscillations experiments. The latter have provided strong evidences for the surface transport even though further work has to be done in order to fully prove the relevance of the Dirac spectrum. The magnetoresistance oscillations with periods of h/e and $h/(2e)$ observed in topological insulator nanoribbons may be associated with the surface states, but they remain to be understood theoretically. A great deal has been learned from the transport measurements of epitaxial TI thin films. The low field magnetoconductivity due to weak antilocalization may become a basis for convenient identification of the surface state transport. The highly tunable TI thin films have been epitaxially grown on $SrTiO_3$ substrates. The high-k dielectric enables the Fermi energy to be pulled from the conduction band to the band gap and even below the Dirac point. Suppression of the bulk conductivity by gating has also been demonstrated, despite that a small amount of residue conductivity of impurity band cannot be completely ruled out. The temperature dependent measurements of the n-doped samples have suggested the importance of the electron–electron interaction effects, but the true surface transport properties remain to be explored in order to confirm the predicted immunity to localization. The advances mentioned above may be treated as a promising starting point for this emerging field. A lot of experimental challenges, including materials synthesis, interface engineering, and device fabrication, have to be addressed in order to observe various novel effects in the topological insulators as well as to realize any possible application.

Acknowledgements We acknowledge valuable contributions from J. Chen, H. J. Qin, X. Y. He, G. H. Zhang, F. Yang, J. Liu, T. Guan, F. M. Qu, C. J. Lin and W. M. Yang, as well as collaborations with L. Lu, Z. Q. Ji, and C. L Yang. We are grateful to X. Dai, Z. Fang, L. Fu, I. V. Gornyi, A. D. Mirlin, V. Sacksteder, J. H. Smet and Y. G. Yao for insightful discussions. This work was supported by the National Natural Science Foundation of China (Grant Nos. 10874210 and 10974240), the State Key Development Program for Basic Research of China (973 Program) (Grant Nos. 2007CB936800 and 2009CB929101), and the Hundred-Talented-Project of the Chinese Academy of Sciences.

References

1. K. von Klitzing, G. Dorda, and M. Pepper, Phys. Rev. Lett., 1980, 45(6): 494
2. M. König, S. Wiedmann, C. Brüne, A. Roth, H. Buhmann, L. W. Molenkamp, X. L. Qi, and S.-C. Zhang, Science, 2007, 318(5851): 766
3. B. A. Bernevig, T. A. Hughes, and S.-C. Zhang, Science, 2006, 314(5806): 1757
4. C. L. Kane and E. J. Mele, Phys. Rev. Lett., 2005, 95(22): 226801
5. C. L. Kane and E. J. Mele, Phys. Rev. Lett., 2005, 95(14): 146802
6. L. Fu, C. L. Kane, and E. J. Mele, Phys. Rev. Lett., 2007, 98(10): 106803
7. J. E. Moore and L. Balents, Phys. Rev. B, 2007, 75(12): 121306(R)
8. R. Roy, Phys. Rev. B, 2009, 79(19): 195322
9. L. Fu and C. L. Kane, Phys. Rev. B, 2007, 76(4): 045302
10. D. Hsieh, D. Qian, L. Wray, Y. Xia, Y. S. Hor, R. J. Cava, and M. Z. Hasan, Nature (London), 2008, 452(7190): 970
11. Y. Xia, D. Qian, D. Hsieh, L. Wray, A. Pal, H. Lin, A. Bansil, D. Grauer, Y. S. Hor, R. J. Cava, and M. Z. Hasan, Nat. Phys., 2009, 5(6): 398
12. Y. L. Chen, J. G. Analytis, J. H. Chu, Z. K. Liu, S.-K. Mo, X. L. Qi, H. J. Zhang, D. H. Lu, X. Dai, Z. Fang, S.-C. Zhang, I. R. Fisher, Z. Hussain, and Z.-X. Shen, Science, 2009, 325(5937): 178

13. P. Roushan, J. Seo, C. V. Parker, Y. S. Hor, D. Hsieh, D. Qian, A. Richardella, M. Z. Hasan, R. J. Cava, and A. Yazdani, Nature (London), 2009, 460(7259): 1106
14. T. Zhang, P. Cheng, X. Chen, J. F. Jia, X. C. Ma, K. He, L. L. Wang, H. J. Zhang, X. Dai, Z. Fang, X. C. Xie, and Q. K. Xue, Phys. Rev. Lett., 2009, 103(26): 266803
15. M. Z. Hasan and C. L. Kane, Rev. Mod. Phys., 2010, 82(4): 3045
16. X. L. Qi and S.-C. Zhang, arXiv:1008.2026, 2010
17. M. Z. Hasan and J. E. Moore, arXiv:1011.5462, 2010
18. A. V. Geim and K. S. Novoselov, Nat. Mater., 2007, 6(3): 183
19. D. Schoenberg, Magnetic Oscillations in Metals, Cambridge: Cambridge University Press, 1984
20. H. Köhler, Phys. Stat. Sol. B, 1973, 58(1): 91
21. H. Köhler, Solid State Commun., 1973, 13(10): 1585
22. H. Köhler and E. Wuechner, Phys. Stat. Sol. B, 1975, 67(2): 665
23. H. Köhler, Phys. Stat. Sol. B, 1976, 73(1): 95
24. H. Köhler, Phys. Stat. Sol. B, 1976, 75(1): 127
25. A. A. Taskin and Y. Ando, Phys. Rev. B, 2009, 80(8): 085303
26. H. J. Zhang, C. X. Liu, X. L. Qi, X. Dai, Z. Fang, and S.-C. Zhang, Nat. Phys., 2009, 5(6): 438
27. L. Fu and C. L. Kane, Phys. Rev. Lett., 2008, 100(9): 096407
28. L. Fu and C. L. Kane, Phys. Rev. Lett., 2009, 102(21): 216403
29. A. R. Akhmerov, J. Nilsson, and C. W. J. Beenakker, Phys. Rev. Lett., 2009, 102(21): 216404
30. Y. S. Hor, A. Richardella, P. Roushan, Y. Xia, J. G. Checkelsky, A. Yazdani, M. Z. Hasan, N. P. Ong, and R. J. Cava, Phys. Rev. B, 2009, 79(19): 195208
31. Y. L. Chen, J.-H. Chu, J. G. Analytis, Z. K. Liu, K. Igarashi, H.-H. Kuo, X. L. Qi, S. K. Mo, R. G. Moore, D. H. Lu, M. Hashimoto, T. Sasagawa, S.-C. Zhang, I. R. Fisher, Z. Hussain, and Z. X. Shen, Science, 2010, 329(5992): 659, and also online supporting materials
32. N. P. Butch, K. Kirshenbaum, P. Syers, A. B. Sushkov, G. S. Jenkins, H. D. Drew, and J. Paglione, Phys. Rev. B, 2010, 81(24): 241301
33. J. G. Analytis, R. D. McDonald, S. C. Riggs, J. H. Chu, G. S. Boebinger, and I. R. Fisher, Nat. Phys., 2010, 6(12): 960
34. M. Bianchi, D. Guan, S. Bao, J. L. Mi, B. B. Iversen, P. D. C. King, and Ph. Hofmann, Nat. Commun., 2010, 1(8): 128
35. J. G. Analytis, J.-H. Chu, Y. L. Chen, F. Corredor, R. D. McDonald, Z. X. Shen, and I. R. Fisher, Phys. Rev. B, 2010, 81(20): 205407
36. D. X. Qu, Y. S. Hor, J. Xiong, R. J. Cava, and N. P. Ong, Science, 2010, 329(5993): 821
37. F. Xiu, L. He, Y. Wang, L. Cheng, L.-T. Chang, M. Lang, G. Huang, X. Kou, Y. Zhou, X. Jiang, Z. Chen, J. Zou, A. Shailos, and K. L. Wang, Nat. Nano., doi:10.1038/nnano.2011.19
38. Z. Ren, A. A. Taskin, S. Sasaki, K. Segawa, and Y. Ando, Phys. Rev. B, 2010, 82(24): 241306
39. J. Xiong, A. C. Petersen, Dongxia Qu, R. J. Cava, and N. P. Ong, arXiv:1101.1315, 2011
40. K. S. Novoselov, A. K. Geim, S. V. Morozov, D. Jiang, M. I. Katsnelson, I. V. Grigorieva, S. V. Dubonos, and A. A. Firsov, Nature (London), 2005, 438(7065): 197
41. Y. B. Zhang, Y. W. Tan, H. L. Stormer, and P. Kim, Nature (London), 2005, 438(7065): 201
42. A. A. Taskin and Y. Ando, arXiv:1103.3096, 2011
43. B. L. Altshuler, A. G. Aronov, and B. Z. Spivak, JETP Lett., 1981, 33: 94
44. Y. Aharonov and D. Bohm, Phys. Rev., 1959, 115(3): 485
45. D. Y. Sharvin and Y. V. Sharvin, JETP Lett., 1981, 34: 272
46. C. Schönenberger, A. Bachtold, C. Strunk, J.-P. Salvetat, J.-M. Bonard, L. Forró, and T. Nussbaumer, Nature (London), 1999, 397(6721): 673
47. H. L. Peng, K. Lai, D. Kong, S. Meister, Y. Chen, X. L. Qi, S.-C. Zhang, Z.-X. Shen, and Y. Cui, Nat. Mater., 2010, 9(3): 225
48. J. H. Bardarson, P. W. Brouwer, and J. E. Moore, Phys. Rev. Lett., 2010, 105(15): 156803
49. Y. Zhang and A. Vishwanath, Phys. Rev. Lett., 2010, 105(20): 206601
50. Y. Y. Qin, Z. G. Li, Z. Qu, Q. H. Wang, W. F. Ding, B. G. Wang, X. F. Wang, C. Van Haesondonck, F. Q. Song, M. Han, Y. H. Zhang, G. H. Wang, and J. G. Wan, arXiv:1012.0104, 2010
51. D. Hsieh, Y. Xia, L. Wray, D. Qian, A. Pal, J. H. Dil, J. Osterwalder, F. Meier, G. Bihlmayer, C. L. Kane, Y. S. Hor, R. J. Cava, and M. Z. Hasan, Science, 2009, 323(5916): 919
52. T. Ihn, Nat. Mater., 2010, 9(3): 187
53. H. Z. Lu, W. Y. Shan, W. Yao, Q. Niu, and S. Q. Shen, Phys. Rev. B, 2010, 81: 115407
54. C. X. Liu, H. J. Zhang, B. H. Yan, X. L. Qi, T. Frauenheim, X. Dai, Z. Fang, and S.-C. Zhang, Phys. Rev. B., 2010, 81(4): 041307(R)
55. G. H. Zhang, H. J. Qin, J. Teng, J. D. Guo, Q. Guo, X. Dai, Z. Fang, and K. H. Wu, Appl. Phys. Lett., 2009, 95: 053114
56. K. He, Y. Zhang, C. Z. Chang, C. L. Song, L. L. Wang, X. Chen, J. F. Jia, Z. Fang, X. Dai, W. Y. Shan, S. Q. Shen, Q. Niu, X. L. Qi, S.-C. Zhang, X. C. Ma, and Q. K. Xue, Nat. Phys., 2010, 6(8): 584
57. Y. Zhang, C. Z. Chang, K. He, L. L. Wang, X. Chen, J. F. Jia, X. C. Ma, and Q. K. Xue, Appl. Phys. Lett., 2010, 97(19): 194102
58. C. L. Song, Y. L. Wang, Y. P. Jiang, Y. Zhang, C. Z. Chang, L. Wang, K. He, X. Chen, J. F. Jia, Y. Wang, Z. Fang, X. Dai, X. C. Xie, X. L. Qi, S.-C. Zhang, Q. K. Xue, and X. C. Ma, Appl. Phys. Lett., 2010, 97(14): 143118
59. J. Chen, H. J. Qin, F. Yang, J. Liu, T. Guan, F. M. Qu, G. H. Zhang, J. R. Shi, X. C. Xie, C. L. Yang, K. H. Wu, Y. Q. Li, and L. Lu, Phys. Rev. Lett., 2010, 105(17): 176602
60. G. H. Zhang, H. J. Qin, J. Chen, X. Y. He, L. Lu, Y. Q. Li, and K. H. Wu, Adv. Func. Mater., DOI: 10.1002/adfm.201002667, 2011
61. H. D. Li, Z. Y. Wang, X. Guo, T. L. Wong, N. Wang, and M. H. Xie, Appl. Phys. Lett., 2011, 98(4): 043104
62. C. Z. Chang, K. He, L. L. Wang, X. C. Ma, M. H. Liu, Z. C. Zhang, X. Chen, Y. Y. Wang, and Q. K. Xue, arXiv:1012.5716, 2010
63. Y. Y. Li, G. Wang, X. G. Zhu, M. H. Liu, C. Ye, X. Chen, Y. Y. Wang, K. He, L. L. Wang, X. C. Ma, H. J. Zhang, X. Dai, Z. Fang, X. C. Xie, Y. Liu, X. L. Qi, J. F. Jia, S.-C. Zhang, and Q. K. Xue, Adv. Mater., 2010, 22(36): 4002
64. H. D. Li, Z. Y. Wang, X. Kan, X. Guo, H. T. He, Z. Wang, J. N. Wang, T. L. Wong, N. Wang, and M. H. Xie, New J. Phys., 2010, 12(10): 103038

65. A. Richardella, D. M. Zhang, J. S. Lee, A. Koser, D. W. Rench, A. L. Yeats, B. B. Buckley, D. D. Awschalom, and N. Samarth, Appl. Phys. Lett., 2010, 97(26): 262104
66. P. Cheng, C. Song, T. Zhang, Y. Zhang, Y. Wang, J. F. Jia, J. Wang, Y. Wang, B. F. Zhu, X. Chen, X. C. Ma, K. He, L. Wang, X. Dai, Z. Fang, X. C. Xie, X. L. Qi, C. X. Liu, S.-C. Zhang, and Q. K. Xue, Phys. Rev. Lett., 2010, 105(7): 076801
67. H. T. He, G. Wang, T. Zhang, I.-K. Sou, G. K. L. Wong, and J. N. Wang, Phys. Rev. Lett., 2011, 106(16): 166805
68. M. H. Liu, C. Z. Chang, Z. C. Zhang, Y. Zhang, W. Ruan, K. He, L. L.Wang, X. Chen, J. F. Jia, S.-C. Zhang, Q. K. Xue, X. C. Ma, and Y. Y. Wang, Phys. Rev. B, 2011, 83(16): 165440
69. J. Wang, A. M. DaSilva, C. Z. Chang, K. He, J. K. Jain, N. Samarth, X. C. Ma, Q.-K. Xue, and M. H. W. Chan, arXiv:1012.0271, 2010
70. J. Chen, X. Y. He, K. H. Wu, Z. Q. Ji, L. Lu, J. R. Shi, J. H. Smet, and Y. Q. Li, arXiv:1104.0986, 2011, to appear in Phys. Rev. B (Rapid Commun.)
71. D. Hsieh, Y. Xia, D. Qian, L. Wray, J. H. Dil, F. Meier, J. Osterwalder, L. Patthey, J. G. Checkelsky, N. P. Ong, A. V. Fedorov, H. Lin, A. Bansil, D. Grauer, Y. S. Hor, R. J. Cava, and M. Z. Hasan, Nature (London), 2009, 460(7259): 1101
72. J. Chen, X. Y. He, K. H. Wu, and Y. Q. Li, unpublished
73. D. S. Kong, J. J. Cha, K. J. Lai, H. L. Peng, J. G. Analytis, S. Meister, Y. L. Chen, H. J. Zhang, I. R. Fisher, Z.-X. Shen, and Y. Cui, arXiv:1102.3935, 2011
74. D. Teweldebrhan, V. Goyal, and A. A. Balandin, Nano Lett., 2010, 10(4): 1209
75. J. G. Checkelsky, Y. S. Hor, R. J. Cava, and N. P. Ong, Phys. Rev. Lett., 2011, 106: 196801
76. D. Kong, W. Dang, J. J. Cha, H. Li, S. Meister, H. Peng, Z. Liu, and Y. Cui, Nano Lett., 2010, 10(6): 2245
77. R. Yu, W. Zhang, H. J. Zhang, S.-C. Zhang, X. Dai, and Z. Fang, Science, 2010, 329(5987): 61
78. X. L. Qi, R. D. Li, J. Zang, and S.-C. Zhang, Science, 2009, 323(5918): 1184
79. I. Garate and M. Franz, Phys. Rev. Lett., 2010, 104(14): 146802
80. H. Steinberg, J. Laloe, V. Fatemi, J. S. Moodera, and P. Jarillo-Herrero, arXiv:1104.1404, 2011
81. H. Steinberg, D. R. Gardner, Y. S. Lee, and P. Jarillo-Herrero, Nano Lett., 2010, 10(12): 5032
82. R. C. Neville, B. Hoeneisen, and C. A. Mead, J. Appl. Phys., 1972, 43(5): 2124
83. D. Caviglia, S. Gariglio, N. Reyren, D. Jaccard, T. Schneider, M. Gabay, S. Thiel, G. Hammerl, J. Mannhart, and J.-M. Triscone, Nature (London), 2008, 456(7222): 624
84. P. M. Ostrovsky, I. V. Gornyi, and A. D. Mirlin, Phys. Rev. Lett., 2010, 105: 036803
85. E. McCann, K. Kechedzhi, V. I. Falko, H. Suzuura, T. Ando, and B. L. Altshuler, Phys. Rev. Lett., 2006, 97(14): 146805
86. The coefficient α would be $4 \times 1/2 = 2$ for graphene if the intervalley and chirality breaking scatterings could be neglected.
87. G. Bergmann, Phys. Rep., 1984, 107(1): 1
88. R. L. Kallaher and J. J. Heremans, Phys. Rev. B, 2009, 79(7): 075322
89. S. Hikami, A. I. Larkin, and Y. Nagaoka, Prog. Theor. Phys., 1980, 63(2): 707
90. H. Hoffmann, F. Hofmann, and W. Schoepe, Phys. Rev. B, 1982, 25(8): 5563
91. O. Rabin, K. Nielsch, and M. S. Dresselhaus, Appl. Phys. A, 2006, 82(3): 471
92. $\alpha \simeq 1/2$ was also obtained previously from Bi_2Se_3 thin films on Si by F. Yang *et al.* (unpublished)
93. Qualitatively similar variation of α with V_G was also reported in Ref. [75], in which the weak antilocalization signal is however superimposed on fluctuating background of unknown origin. The non-Hall-bar device-geometry also precluded accurate determination of α in that work.
94. M. Kawasaki, K. Takahashi, T. Maeda, R. Tsuchiya, M. Shinohara, O. Ishiyama, T. Yonezawa, and H. Koinuma, Science, 1994, 266: 1540
95. A. A. Abrikosov, Phys. Rev. B, 1998, 58(5): 2788
96. M. M. Parish and P. B. Littlewood, Nature, 2003, 426(6963): 162
97. H. Tang, D. Liang, R. L. J. Qiu, and X. P. A. Gao, arXiv:1003.6099, 2010
98. P. A. Lee and T. V. Ramakrishnan, Rev. Mod. Phys., 1985, 57(2): 287
99. B. L. Altshuler and A. G. Aronov, in: Electron-Electron Interactions in Disordered Systems, edited by A. L. Efros and M. Pollak, Amsterdam, North-Holland, 1985
100. B. L. Altshuler, A. G. Aronov, and A. Y. Zuzin, Solid State Commun., 1982, 44(2): 137
101. A. Sahnoune, J. O. Strom-Olsen, and H. E. Fischer, Phys. Rev. B, 1992, 46(16): 10035
102. A. M. Finkelstein, Sov. Sci. Rev. A, 1990, 14: 1
103. D. Belitz and T. R. Kirkpatrick, Rev. Mod. Phys., 1994, 66(2): 261
104. A. D. Mirlin, private communications